Chemistry & Biology 13, 869–879, August 2006 DOI 10.1016/j.chembiol.2006.06.011

Interdomain Communication between the Thiolation and Thioesterase Domains of EntF Explored by Combinatorial Mutagenesis and Selection

Zhe Zhou,[1] Jonathan R. Lai,[1] and Christopher T. Walsh[1,*]
[1] Department of Biological Chemistry and Molecular Pharmacology
Harvard Medical School
240 Longwood Avenue
Boston, Massachusetts 02115

Summary

Thiolation (T) domains are protein way stations in natural product assembly lines. In the enterobactin synthetase, the T domain on EntF is recognized in cis by its catalytic partners: the EntF condensation (C), adenylation (A), and thioesterase (TE) domains. To assess surface features of the EntF T domain recognized by C, A, and TE, regions of the EntF T domain were submitted to shotgun alanine scanning and Ent production selection, which revealed residues that could not be substituted by Ala. EntF mutants bearing Ala in such positions were assayed in vitro for Ent production with EntEB, and for A-T, C-T, and T-TE communications. We concluded that G1027A and M1030A are specifically defective in acyl transfer from T to TE. These residues define an interaction surface between these two in cis domains in an NRPS module.

Introduction

Polyketides (PKs) and nonribosomal peptides (NRPs) are two classes of pharmaceutically interesting natural products that are biosynthesized by large, multimodular enzymes known as polyketide synthases (PKSs) and nonribosomal peptide synthetases (NRPSs) [1]. Examples of important PK and NRP compounds include the antibiotics erythromycin (PK) [2], rifamycin (PK) [3], and vancomycin (NRP) [4], the immnosuppresants FK506 (PK) [5] and rapamycin (hybrid PK/NRP) [6], and the antitumor agents epothilone [7] and bleomycin (both are hybrid PK/NRP) [8].

Central to the multidomain architecture of PKSs and NRPSs are carrier proteins, autonomously folding domains of 80–100 amino acid residues (8–10 kDa) that carry the growing acyl or peptidyl chains during substrate elongation cycles [9]. Carrier proteins from PKS assembly lines have been termed acyl carrier proteins (ACPs), and those from NRPSs have been termed peptidyl carrier proteins (PCPs); both are homologous to the ACPs from primary metabolism (fatty acid synthases, FASs). Because ACP and PCP domains require posttranslational priming to become active, by installation of a phosphopantetheinyl prosthetic group whose terminal thiol becomes the site of covalent tethering of growing acyl chains, the ACP and PCP domains are often referred to as thiolation (T) domains to emphasize the pantetheinyl thiol functionality [9]. This convention is used here.

In type I synthases/synthetases, with multiple domains organized into monomer-processing modules and up to eight modules per protein subunit, a T domain is embedded in each module and is serviced in cis by the adjacent catalytic domains [10–12]. In type II FAS, PKS, and NRPS multienzyme systems, the T domains are most often free-standing subunits, interacting in trans with catalytic partners [11, 13, 14]. Whether in cis or in trans, the multiple cycles of loading and elongation that result in production of the growing acyl or peptidyl chain require that T domains participate in well-timed communication events with the domains that activate the monomer to be incorporated (adenylation domains, A, in NRPSs and acyl transferase domains, AT, in PKSs) and the domains that catalyze chain elongation (condensation domains, C, and ketosynthase domains, KS) [15, 16]. In addition, the T-domain-tethered substrates can undergo various modifications, such as oxidation [17], methylation [18], epimerization [19], and halogenation [20]. Therefore, a great amount of information is encoded in the 8–10 kDa T domains for directing enzymatic reactions in a spatially and temporally controlled fashion.

The siderophore enterobactin, produced by gram-negative enteric bacteria in times of iron starvation, is a cyclic trilactone comprised of three *N*-(2,3-dihydroxybenzoyl)-serine (DHB-Ser) residues [21]. The DHB moieties in enterobactin provide three catecholic groups to form a high affinity hexadentate complex with ferric iron. Enterobactin is assembled by the two module NRPS enterobactin synthetase [22], spreading over three proteins EntEBF. EntE is a DHB-selective adenylation domain, EntB is a two-domain protein, one domain of which is a free-standing T domain, and EntF is a four-domain NRPS elongation/termination module (C-A-T-TE) [23–27]. The EntEB pair functions together as a type II NRPS, while the EntF module has type I organization. The A domain of EntF activates L-Ser and installs it on the phosphopantheine free thiol of the EntF holo-T domain [27]. The C domain condenses the DHB acyl group (presented as the thioester tethered to EntB via its phosphopantetheine group, DHB-*S*-EntB) onto the amino group of Ser-*S*-EntF [28]. Finally the TE domain of EntF acts as an elongation and cyclotrimerization catalyst, releasing the trilactone siderophore [29]. A scheme for the catalytic steps for enterobactin production is shown in Figure 1A.

The two T domains in the Ent assembly line thus reflect the two distinct contexts, in cis versus in trans, for recognition by partner domains. Ample evidence exists from natural product assembly lines with in trans components that many T domains are differentiated by potential partner catalytic domains. An example of this, T domain selectivity is demonstrated by the PKS systems that produce frenolicin (FrnN/J) and R1128 (ZhuG/N) [30]. Only cognate pairwise interactions of T domains and KSs occur in both initiation and elongation cycles of these type II synthases. In the NRPS system for coronatine production, the nonheme iron halogenase

*Correspondence: christopher_walsh@hms.harvard.edu

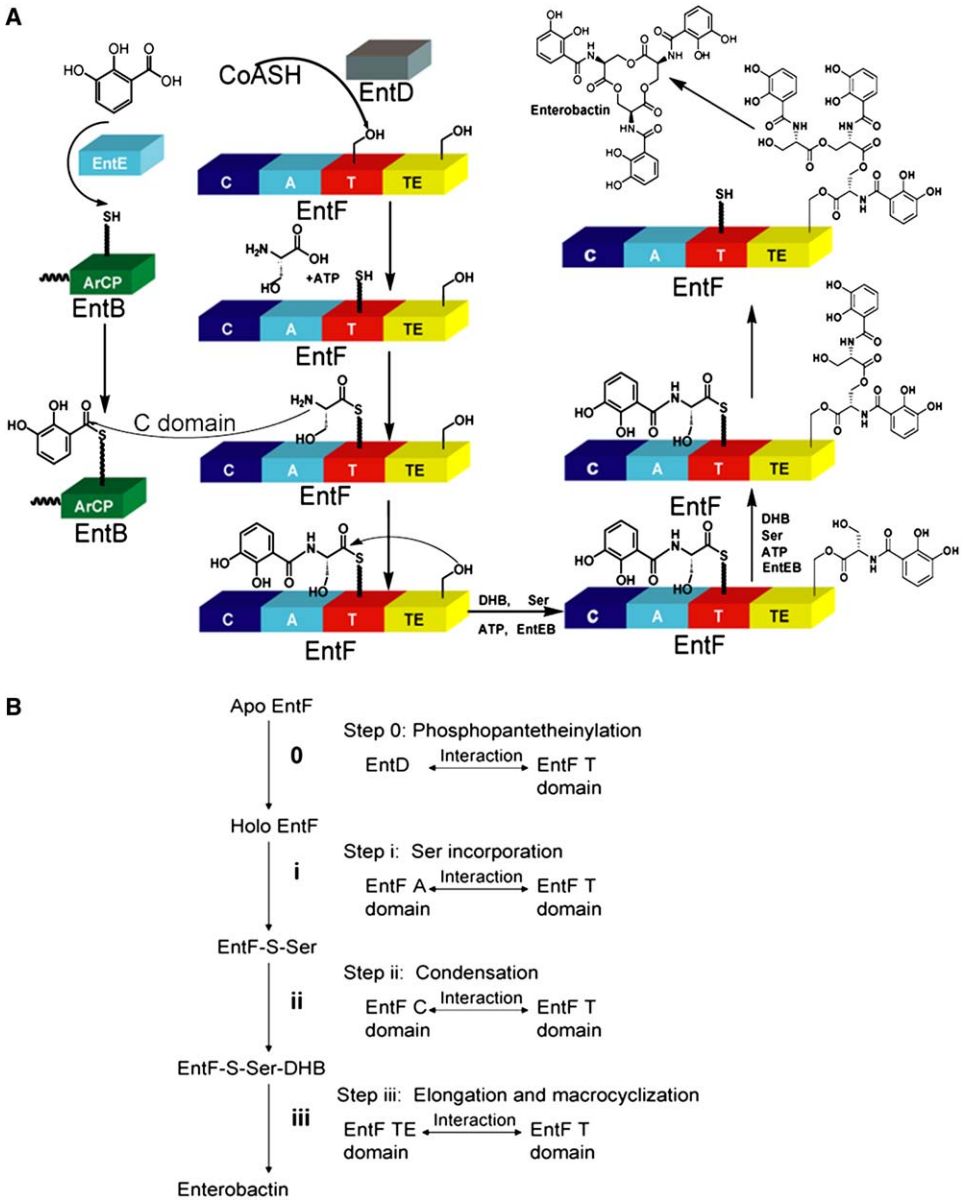

Figure 1. Enterobactin Biosynthesis Scheme

(A) EntD is a PPTase that primes EntB and EntF. EntE loads DHB onto holo-EntB-ArCP. EntF is a four-domain NRPS elongation/termination module (C-A-T-TE). The A domain of EntF catalyzes loading of the T domain with Serine. The C domain then mediates condensation of Serine with DHB loaded on EntB ArCP. The TE domain elongates DHB-Ser and macrocyclizes the DHB-Ser trimer to form enterobactin.

(B) The cascade of enterobactin biosynthesis reactions that involve the EntF T domain. The interdomain interactions that must occur for each step are shown.

that installs a chlorine group onto alloisoleucine (CmaB) recognizes the alloisoleucine substrate only when presented on the T domain of CmaD but not CmaA [20]. It has been much more difficult to evaluate whether in cis T domains of NRPS modules have such specific recognition by their juxtaposed neighboring catalytic domains.

In any prototypic enzymatic assembly line, there are chain initiation, elongation, and termination cycles [1]; in type I NRPS systems, these would comprise an A-T module, a C-A-T module, and a C-A-T-TE module, respectively. In an initiation module the T domain must be recognized by: (1) the dedicated phosphopantetheinyl transferase (PPTase) that primes it from inactive apo to the active holo form; (2) the A domain that selects, activates, and loads a specific acyl/aminoacyl group on the holo-T domain; (3a) the downstream C domain in the first elongation module that catalyzes bond formation between the activated initiation acyl/aminoacyl group and the downstream amino acid. In elongation modules there is: (4) recognition of an acyl/aminoacyl-*S*-T domain by both the upstream as well as the downstream C domains during a condensation/chain transfer step. Finally, when the full-length acyl chain has reached the termination module, the downstream C domain is typically replaced by the TE domain; this scenario would

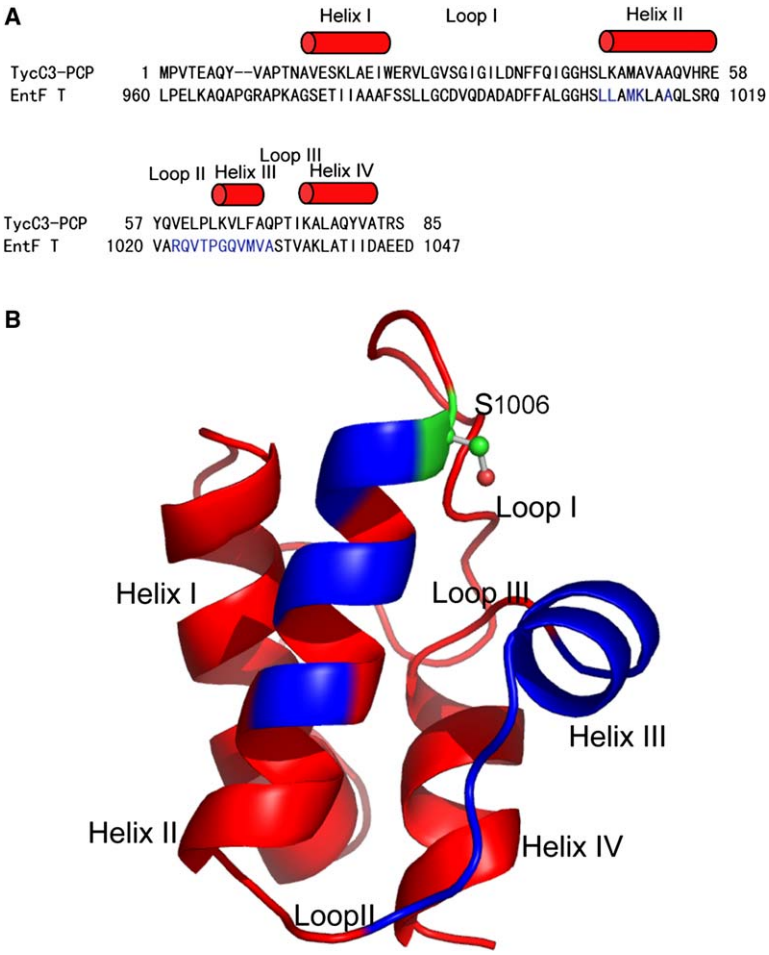

Figure 2. Homology Model of the EntF T Domain

(A) Sequence alignment of the EntF T domain with TycC3-PCP that was used for generation of the EntF T domain homology model.

(B) Ribbon diagram of the homology model of EntT T domain. Residues of EntF T domain that were subjected to shotgun alanine scanning are shown in blue.

be variation (3b) in the list above. Thus, a T domain in a termination module might have a recognition face for TE but not a downstream C domain, or there could be equivalent sites for interaction with TE or C.

In the two-module EntEBF system EntEB acts as initiation module, while EntF functions as both an elongation and a termination module. Given that the four-helix T domain scaffolds can be distinguished, at least by some partner proteins that work in trans, we have recently begun to determine if the EntB T domain presents different faces to its distinct partners, EntD (the PPTase), EntE (the A domain), and EntF (C domain). We employed a selection under low iron conditions where *E. coli* require the capacity to produce enterobactin to grow on low iron media [31]. By combinatorial mutagenesis of selected regions on EntB, we identified a surface of the EntB T domain that, upon mutation in the comprising residues, was specifically impaired for recognition by the EntF elongation module but not interaction with EntD or EntE.

In the current study, we have turned to the in cis T domain of the 142 kDa protein EntF to assess comparable libraries by combinatorial mutagenesis. We sought to determine if there might be analogous selection for maintenance/loss of enterobactin synthesis that could be mapped onto a specific recognition surface of one of the EntF domains and in cis and in trans contexts from the same assembly line compared.

Results

Homology Modeling of the EntF T Domain and Library Design

Carrier protein domains are approximately 80 to 100 residues in length. A structure of the EntF T domain is not currently available; we therefore produced a structural model based on homology with a T domain from the tyrocidine NRPS system (TycC3-PCP) [32]. Residues 960–1047 of EntF were aligned with TycC3-PCP by using the ClustalW algorithm (Figure 2A). The EntF T domain shares 30% sequence identity with TycC3-PCP (this value is higher than the sequence identity that the EntF T domain shares with the EntB T domain), which suggests that these two carrier proteins should have similar folds. Indeed, several carrier proteins from primary or secondary metabolism have been shown to adopt three- or four-helix bundle structures similar to that of TycC3-PCP. Using the TycC3-PCP NMR structure as template, we generated a structural model of the EntF T domain. The EntF T domain model is shown in Figure 2B. As with other carrier proteins, our EntF T domain homology model is comprised of a four-helix bundle structure. A long loop links helix I and helix II, a short loop connects helix II and helix III, and an even shorter loop is found between helix III and helix IV. The site of phosphopantetheinylation, Ser1006, is located at the N-terminal end of helix II.

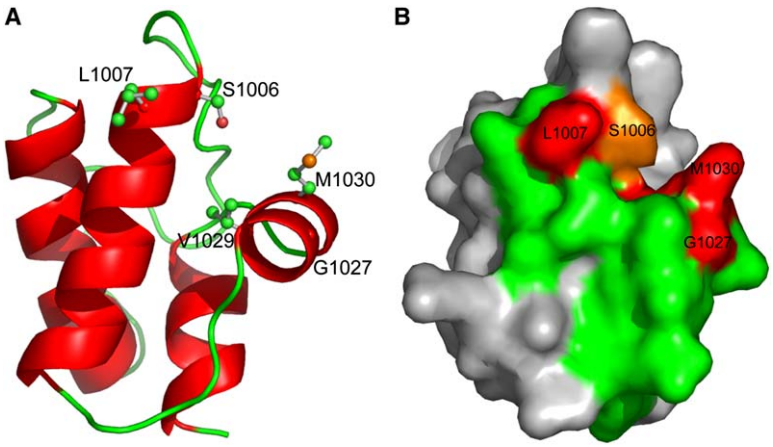

Figure 3. Conserved Residues from Combinatorial Mutagenesis and Selection

Ball and stick (A) and surface (B) representation of residues on the EntF T domain model that were highly conserved in the iron-deficient selection. In the surface representation, the conserved residues are shown in red, the nonconserved residues are shown in green, the phosphopantetheinlyated Ser is shown in yellow, and unscanned residues are shown in gray.

Helix II of the *B. subtilis* ACP from primary metabolism has been reported to be important for interaction of the ACP with its cognate phosphopantetheinyl transferase ACPS (ACP synthase) [33]. Also, helix II residues on PCPs have been reported to mediate interaction with catalytic partners [34]. We have recently shown that residues in helix III of EntB-ArCP constitute an interaction interface for the downstream elongation module, EntF [31]. Therefore, we targeted these portions on the EntF T domain surface (predicted to lie in the helix II/loopII/helixIII region) for combinatorial mutagenesis via shotgun alanine scanning. In this combinatorial mutagenesis strategy, codons are used that allow the residues to vary between wt, Ala, and sometimes a third or fourth residue [35]. For cases where the wt residue was Ala, we used a combinatorial codon set that allowed the side-chain identity to vary between Ala, Glu, Gln, Pro. Three libraries spanning regions of helix II, helix III, and loop II/helix III were prepared (Figures 2A and 2B). The theoretical sequence diversity for the three libraries (1024, 256, and 256 for helix II, helix III, and loopII/helixIII, respectively) were adequately represented among our total clones for each library (2×10^3 for helix II, 1×10^3 for helix III, and 5×10^2 for loopII/helix III).

In Vivo Selection for Enterobactin Production

Selection for functional EntF clones was based on the fact that enterobactin production is essential for the survival of *E. coli* under low iron conditions. The *E. coli* strain *entF::cat* (ER 1100A) contains a chromosomal replacement of the *entF* gene by a chloramphenicol resistance marker [28]. We previously reported that the *entF::cat* strain is not able to grow in minimal media in which iron is sequestered by the chelator 2,2′-dipyridyl. However, the *entF* knockout cells could be complemented by transformation with a pET29-based plasmid that harbors the wild-type *entF* gene [28]. We recently described the use of a similar complementation and selection format to quickly assess many variants of EntB for their ability to support growth of an *entB* knockout strain on iron-deficient media [31].

Bacteria harboring the EntF libraries were subjected to the iron-deficient selection conditions. Colonies of varying sizes were observed after 24 hr at 37°C, the largest of which were isolated and sequenced. Twenty-nine, 16, and 17 nonredundant surviving clones from the helix II, helix III, and loop II/helix III libraries (respectively) were analyzed. Further sequencing of survival colonies from helix III and loop II/helix III (40 and 44 total colonies sequenced, respectively) yielded redundant sequences. This result might be due to the small sequence diversity of these two libraries. The survival rate on selection medium was estimated by comparing numbers of colonies that grew on rich media with the number of colonies that grew on low-iron media. We observed survival rates of 30% for the helix II library, 8% for the helix III library, and 15% for the loop II/helix III library.

For residues L1007, G1027, V1029, and M1030, the wt amino acid was strongly preferred over Ala (no Ala residues were observed in surviving clones at these positions (Table S1; see the Supplemental Data available with this article online). The residue V1029 is predicted to be a core residue in the EntF T domain homology model; furthermore, NMR studies of an EntF fragment confirmed that V1029 points toward the core of the EntF T domain (D. Frueh, D. Vosburg, C.T.W., G. Wagner, unpublished data). We therefore reasoned that mutation of V1029 would be likely to cause disruption of the EntF T domain structure, and thus we did not characterize any point mutants at this position. Residue L1007 is located on helix II of the EntF T domain homology model, immediately C-terminal to the phosphopantetheinylated Ser. The analogous position was found to be important for interactions between the PPTase and ACP of the *B. subtilis* FAS [33]. Therefore, we predicted that mutation of L1007 may affect posttranslational modification of EntF. The residues G1027 and M1030 lie on helix III of the EntF T domain model. A representation of the EntF T domain homology model with the locations of the conserved residues is shown in Figures 3A and 3B. Based on the above sequence analysis, we expressed and purified wild-type EntF along with several variants that contained single mutations in the T domain: L1007A, G1027A, and M1030A. Expression of EntF (wt and mutants) and the other synthetase components proceeded in good yield and purity by using established protocols.

From the sequencing results for the survivors, it was observed that proline was prohibited within α-helical regions, except at the beginning of helix III. Proline is an α helix-breaking residue and would likely disrupt the structure of the EntF T domain if placed in the middle of an α helix. The observation that proline was not

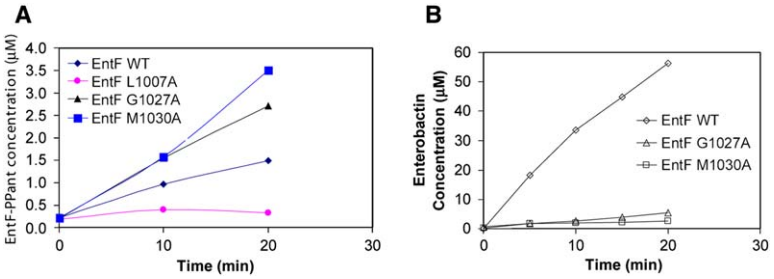

Figure 4. Initial Characterization of EntF T Domain Mutants

(A) Phosphopantetheinylation of EntF T domain (wt and mutants) by EntD. Time courses of radiolabeled holo-EntF production are shown.

(B) Time courses for enterobactin production for EntF (wt and mutants).

observed in α-helical positions of the EntF T domain (where proline was permitted as an option) suggests that *E. coli* survival under low iron conditions is tightly coupled to EntF function. This result indicates that under low iron conditions, *E. coli* are under selective pressure for well-folded and functional EntF variants and therefore confirms that the information from sequencing results will be valuable for dissecting EntF function.

Phosphopantetheinylation Assay

Enterobactin production by the Ent synthetase requires that the T domains of EntB and EntF be primed with the 4′-phosphopantetheine prosthetic group. Two endogenous PPTases are found in *E. coli*: one for primary metabolism (ACPS) and the dedicated PPTase EntD, which is encoded in the enterobactin biosynthetic gene cluster [36]. The PPTase ACPS is responsible for the modification of ACP for fatty acid synthesis but does not accept the EntF T domain as a substrate. However, expression of EntD is upregulated in response to low iron conditions, resulting in the posttranslational modification of the EntB and EntF T domains to their holo forms [25].

In order to determine whether the observed conservation of L1007, G1027, and M1030 during in vivo enterobactin production selection was due to recognition defects between EntF and EntD, a phosphopantetheinylation assay was performed with EntD and EntF (wt and mutants). Figure 4A shows the initial rate of radiolabeled [^{3}H] coenzyme A incorporation into apo-EntF and mutants catalyzed by EntD. We found that wt EntF and the T domain mutants G1027A and M1030A were phosphopantetheinylated by EntD. Surprisingly, these two mutants (G1027A and M1030A) were phosphopantetheinylated at a higher rate than wt EntF. The reason for this elevated rate of phosphopantetheinylation is not clear. However, the apo-EntF L1007A mutant was not accepted as a substrate for EntD, suggesting that L1007, located immediately adjacent to the phosphopantetheinylated serine in the homology model, is important for recognition by EntD. Furthermore, we found that L1007A could not be recognized by the broad-substrate PPTase Sfp from *B. subtilis* (data not shown). The defect in recognition of L1007A by EntD rationalizes the observed conservation of wt side chain identity in the in vivo selection. Interestingly, the aligning residue of the ACP from the *B. subtilis* FAS has been shown to be important for recognition by its cognate PPTase ACPS [33]. Since L1007A could not be phosphopantetheinylated (and therefore could not be converted to the active form), we did not pursue further biochemical characterization of this mutant. However, both G1027A and M1030A could be efficiently recognized by EntD, indicating that the conservation of these residues was not due to the participation of these residues in interactions with EntD.

In Vitro Reconstitution of Enterobactin Biosynthesis

We characterized the mutants G1027A and M1030A in a previously reported enterobactin reconstitution assay involving EntE and EntB [37]. This assay allows validation of the sequence results from combinatorial mutagenesis and affords the opportunity to quantitatively evaluate the overall competence of the EntF mutants for the three steps of the enterobactin biosynthesis reaction cascade (shown in Figure 1B). These three steps are: (1) Ser loading, (2) condensation of Ser with DHB (each substrate is tethered to the appropriate T domain), and (3) elongation and macrocyclization. The three reactions are directed by in cis interactions between EntF domains (A-T for loading, C-T for condensation, and T-TE for elongation and macrocyclization).

To prepare the holo form of EntF (wt and mutants), we used the broad-substrate PPTase Sfp from *B. subtilis*. We found that both mutants could be efficiently phosphopantetheinylated by Sfp. Since the K_m for DHB-*S*-EntB-ArCP as the substrate of EntF is approximately 1 μM, reconstitution assays were preformed at 15 μM EntB-ArCP so that catalysis involving EntF would be the rate-limiting step in enterobactin production. This condition allowed us to evaluate whether the EntF mutants were deficient in any of the in cis interactions listed above.

The production of enterobactin is shown in Figure 4B, and the calculated initial rates of enterobactin production are listed in Table S2. The mutants G1027A and M1030A had lower initial rates of enterobactin production than wt EntF, by 15- and 30-fold, respectively. These results confirm that mutation of these two residues deleteriously affects the enterobactin synthetase and correlates with the observed sequence conservation data. Since both G1027A and M1030A could be phosphopantetheinylated by Sfp (used in this assay), the precise mechanism for the defect in enterobactin production displayed by these mutants must be due to deficiencies in the (1) Ser incorporation step, (2) the condensation step, (3) the elongation and macrocyclization step, or combinations thereof. Each of these steps requires a separate interdomain communication event with the in cis EntF T domain (Figure 1B). We therefore conclude that these mutations affect in cis interdomain interactions such that they hinder function of the EntF module.

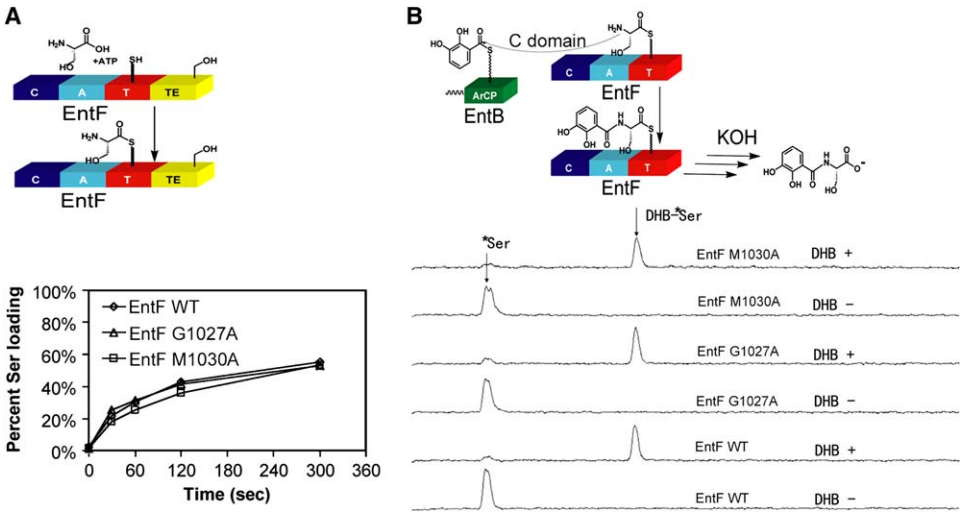

Figure 5. Characterization of A-T and C-T Domain-Domain Interactions for the EntF T Domain Mutants G1027A and M1030A

(A) Time course for [^{14}C]-Ser incorporation onto EntF (wt and mutants).

(B) Radio-HPLC analysis of DHB-Ser condensation products on tridomain C-A-T constructs. The EntF tridomains (wt and mutants) were preloaded with Ser and DHB were added to start the condensation reaction in the presence of EntEB. Protein bound Ser or DHB-Ser were released by KOH treatment.

Loading of Ser onto the EntF T Domain

The loading of Ser onto EntF T domain by the EntF A domain is a two-step process. First, Ser is adenylated by the A domain to form the activated Ser-*O*-AMP ester. Second, this activated Ser-*O*-AMP species is coupled to the thiol on the phosphopentetheinyl arm of the EntF T domain. In order to examine the kinetics of Ser covalent loading onto the EntF T domain, the time course for loading of ^{14}C labeled serine was determined (Figure 5A). For wt EntF, rapid incorporation of radiolabeled serine was observed within 5 min. Neither G1027A nor M1030A displayed a significant difference in the rate of serine loading relative to wt EntF. These observations suggest that the G1027A and M1030A mutations do not disrupt enterobactin synthesis at the serine loading step. Furthermore, we conclude that these residues are not involved in communication between EntF T domain and the EntF A domain.

Condensation Assay

Following the loading of serine onto the EntF T domain, the C domain of EntF catalyzes the condensation of DHB (loaded on EntB-ArCP) with the serine loaded on the EntF T domain to form a DHB-Ser condensation product (Figure 5B). In order to compare the ability of the EntF wt and mutants to perform the condensation between DHB (presented on EntB) and Ser without artifacts arising from transfer of DHB-Ser to the adjacent TE domain or release of DHB-Ser by TE, we produced the EntF C-A-T tridomain proteins for wt, G1027A, M1030A. These C-A-T constructs lack the TE domain, and therefore condensation should be a single turnover event with DHB-Ser accumulating as the covalently bound thioester on the T domain phosphopantetheine group.

In order to facilitate detection, radiolabeled [^{14}C] Ser was employed; reaction products tethered to the T domain of EntF (wt and mutants) were released by treatment with KOH and analyzed on an HPLC equipped with tandem UV and radioactivity detectors. As shown in Figure 5B, complete conversion from of Ser to DHB-Ser was observed for wt and both mutants within 15 s of initiation of the reaction by adding DHB. These data suggest that condensation is a rapid process and that the EntF mutants G1027A and M1030A are not deficient in their ability to catalyze condensation between DHB and Ser. These results further suggest that the in cis communication between the EntF T domain and the EntF C domain is not adversely affected by mutation of G1027 and M1030. At this time, we do not have any biochemical evidence that suggests that the in trans interaction between EntB and EntF involves any portion of the EntF T domain. The results of the DHB-Ser condensation assay with the C-A-T tridomains for both wt and mutants show that these mutations do not affect any interaction between the EntF T domain and EntB that might exist.

Acyl-Transfer from the T Domain to the TE Domain

The EntF TE domain is a unique thioesterase because it is responsible for elongation (trimerization of DHB-Ser via the sidechain hydroxyl of Ser) followed by macrocyclization and release of the mature enterobactin product. This process requires well-timed communication events between the T and TE domains. From the enterobactin reconstitution assay, we concluded that the overall competence of the mutants G1027A and M1030A for the three steps involved in enterobactin production ([1] Ser loading, [2] condensation, and [3] elongation/macrocyclization) was reduced by 15- and 30-fold, respectively. However, neither of these mutations had defects in the Ser loading step or the condensation step as judged by assays that tested each of these steps separately. Therefore, we infer that G1027A and M1030A must be defective in the macrocyclization step (i.e., communication between the T and TE domains of EntF). A direct assay for T-TE communication using

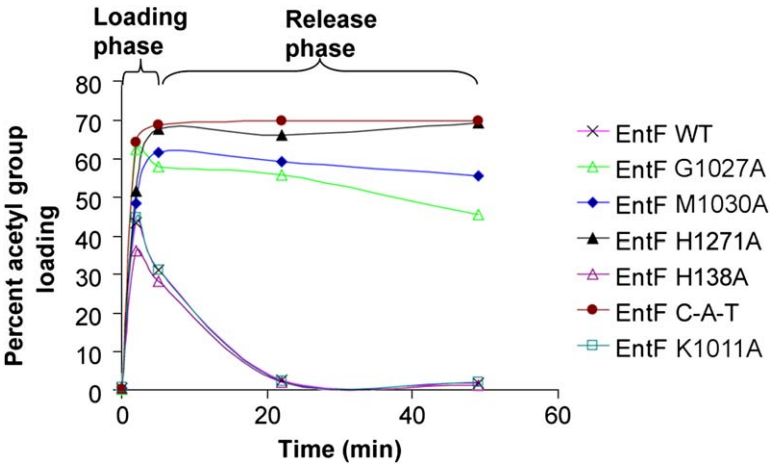

Figure 6. Acyl-Transfer Assay for T-TE Interaction

The PPTase Sfp was used to load 1-[^{14}C]-acetyl-pantetheine onto the T domain (loading phase). In wild-type EntF, this acyl group is transferred to the downstream TE domain and 1-[^{14}C]-acetyl-*O*-TE is hydrolyzed to liberate [^{14}C]-acetate (release phase). When T-TE interaction is impaired, the covalent label remains stably incorporated.

the native DHB and Ser substrates is not available, since it would require loading of three molecules of DHB-Ser individually in proper time series onto the active site serine of the TE domain.

In an effort to determine if the T-TE communication in the G1027A and M1030A EntF mutants were indeed impaired, we developed an assay to examine transfer of an independently primed acyl group from the T domain to the TE domain of EntF. In this assay, T-TE communication was detected by monitoring the net hydrolysis of a noncognate acyl group from EntF. In particular, a limiting amount of 1-[^{14}C]-acetyl-CoA was used with Sfp to load the apo form of EntF (wt and mutants) with 1-[^{14}C]-acetyl-pantethene onto the T domain. In wt EntF, this radiolabeled acyl group is transferred to the active site serine of the downstream TE domain but is not capable of participating in macrocyclization. As shown in Figure 6, the 1-[^{14}C]-acetyl-*O*-TE was hydrolyzed to liberate [^{14}C]-acetate. This phenomenon was manifested as an initial increase in the incorporation of radiolabel (loading catalyzed by Sfp) followed by a loss of the label over time (corresponding to hydrolysis of the radiolabeled acetyl group by the TE domain of EntF). The hydrolysis of acyl-*O*-TE intermediates is the default behavior of many TE domains in NRPS assembly lines [38]. For the mutants G1027A and M1030A, the covalent label remains stably incorporated, consistent with a failure to be transferred to the TE domain for hydrolysis.

Two additional types of controls were performed to further validate that this assay indeed examined the T-TE interaction, shown in Figure 6. The first control utilized the C-A-T tridomain construct of EntF (with the wild-type sequence in the T domain). The 1-[^{14}C-]-acetyl-*S*-T intermediate was stable for the wt tridomain, as expected if hydrolysis requires passage to the TE domain for its catalyzed hydrolysis activity. In the second control, an EntF mutant was assayed in which the histidine in the TE active site that acts as general base was altered (EntF H1271A) [29]. When primed with 1-[^{14}C]-acetyl-pantetheinyl prosthetic group, the EntF TE domain mutant H1271A also did not show the time-dependent loss of radiolabel that was observed with wt EntF. These results indicate that the catalyzed loss of the radioactive acetyl group is dependent on a functional TE domain for EntF. Finally, mutations elsewhere in EntF, H138A in the C domain and K1011A in the T domain, expected to be functional in acyl transfer from T to TE domain, undergo acetyl group hydrolysis (Figure 6). These results indicate that mutations elsewhere in EntF, which are not expected to affect T-TE domain communication, display behavior similar to wt in this assay. Overall, these results suggest that the loss of the acetyl radiolabel under these conditions provides insight into T-TE communication; and furthermore that the T-TE interaction is deficient in the EntF mutants G1027A and M1030A.

Discussion

The T domains that are the centerpiece of the covalent attachment strategy for PKS and NRPS assembly line logic must first be primed by dedicated PPTases that add the 20 Å phosphopantetheine arm, thereby installing the nucleophilic thiol and bringing the assembly lines to the ready position. The thiols of the thiolation domains in turn capture acyl chains in covalent thioester linkage during natural product chain growth. The structure of a number of T domains, of both the ACP and PCP subcategories, have been determined by NMR and/or X-ray in both apo and holo forms [32, 33, 39–44] and show a three- or four-helix scaffold with the Ser residue to be primed with phosphopantetheine near the N-terminal end of helix II. Priming by PPTase requires the folded architecture of the apo-T domains for modification to proceed.

Despite the very similar folds among the 80–100 residue T domains, they can exist in several contexts. One major subgroup is that of free-standing T domains in type II PKS systems such as the actinorhodin, and the frenolicin synthases [40, 45]. At the other extreme are type I PKSs, such as deoxyerythronolide B synthase and rapamycin synthase [2, 46], where a T domain is embedded in cis in every module. Most NRPS assembly lines follow type I assembly logic, e.g., ACV synthetase, tyrocidine synthetase, and the three subunit heptapeptide synthetase in vancomycin construction [4, 47, 48]. However, in coumermycin formation, there is a free standing A and T domain for channeling proline down that antibiotic pathway [49]. The EntEBF synthetase is a hybrid of type I (EntF) and type II (EntBE) contexts with one T domain (EntB) in trans and one T domain (EntF) in cis.

Recent efforts from our group have been directed at approaches to define surfaces of T domains that may be docking areas for protein-protein recognition and to evaluate whether different catalytic partner proteins recognize different faces of T domains [31]. In addition to basic definition of T domains as information-rich protein scaffolds, somewhat akin to the use of ubiquitin as an information-rich scaffold for protein trafficking in eukaryotic cells [50], such knowledge would also aid in successful domain swaps to reprogram natural product assembly lines. We began in previous work with the EntB T domain [31] because we estimated that analysis of in trans recognition by EntD, EntE, and EntF would be more straightforward than the in cis interactions of the T domain embedded within EntF. We were able to isolate mutants where the recognition of the EntB T domain by the downstream C domain of EntF was defective, allowing assignment of that surface to interaction with EntF C domain but not with EntD or EntE and establishing facial selection on the T domain scaffold [31].

Here, we have turned to the other T domain in the Ent synthetase, which is embedded within the four domain EntF and have used the same approach of shotgun alanine scanning and selection for survivors on low iron medium. We kept side chains of core residues in the EntF T domain constant and varied surface residues on helices II and III and in corresponding loops. The positions L1007, G1027, and M1030 could not be mutated to Ala without impaired enterobactin production. The L007A, G1027A, and M1030A mutants of EntF were constructed, purified, and assayed in vitro to validate the defect in Ent formation and to determine which of the domain-domain interactions was affected. First, the priming from apo-EntF to the holo form of the T domain still occurs in G1027A and M1030A but not L1007A. This assay provided a readout that the architecture of the T domain in the vicinity of the critical Ser to be primed is in a native state, and the results indicated that G1027A and M1030A were still competent in this regard, but L1007A was not. Second, the A domain within G1027A and M1030A still activates Ser and installs it on the holo form of the T domain as assayed by covalent loading of radiolabeled Ser onto EntF. The C domain was assayed in truncated three-domain C-A-T constructs of G1027A and M1030A with ^{14}C-labeled Ser and unlabeled DHB with EntE and EntB. In the absence of a TE domain, if the C domain is functioning, it should transfer DHB from DHB-S-EntB to [^{14}C]-Ser-S-EntF and yield the DHB-[^{14}C]-Ser-S-EntF. Cleavage of the thioester allowed detection and quantitation of DHB-[^{14}C]-Ser. Both the G1027A and M1030A forms of EntF were as active as wild-type EntF in this assay, suggesting recognition of the T domain mutants by the C domain in cis was unaffected.

With the C and A domains of EntF unaffected, the most likely effect of the G1027A and M1030A mutations in the EntF T domain are in its recognition by the in cis downstream TE domain. A result consistent with the impairment of T-TE interaction was obtained in an acyl transfer assay. EntF was primed with 1-[^{14}C]-acetyl-CoA. Wild-type EntF hydrolyzes the acetyl thioester, presumably by transfer to the adjacent TE domain, which then acts as an acetyl-thioesterase. The half-life for acetyl group hydrolytic release is about 5 min. Compared to normal enterobactin cyclotrimerization of 100 min^{-1} [29], the hydrolysis of the noncognate acetyl group occurs at about 1/500th the rate, slow enough to be inconsequential for normal turnover but useful as an assay for a slow default hydrolytic activity of EntF TE domain. The G1027A and M1030A mutants in EntF can be stably primed with the acetyl-S-pantetheine consistent with failure to transfer the acetyl group from T to TE.

Both of the T domains in EntB and EntF have surface patches that are loci of specific recognition by particular partner enzymes. In the EntB T domain, two residues on helix III (F264 and A268) and one on helix II (M249) interact with the downstream EntF and are critical for C domain function [31] (Figure 7A). The EntF C domain is the immediate downstream catalytic domain that mediates DHB transfer from the EntB T domain scaffold. In the EntF T domain, the G1027 and M1030 are likewise on helix III and also are recognized by the immediate downstream catalytic domain, in this case the TE domain (Figure 7B).

So far it is not known whether T domains similarly use helix III residues to interact with immediate downstream C domain in cis (Figure 7C). We think it likely that T domains use helix III as a general interaction surface for immediate downstream domains (TE domain in cis, C domain in cis or in trans). Recent structure analysis of the PCP from the third module of the tyrocidine synthetase TycC3-PCP has revealed the conformational motions that can mediate protein interactions in NRPS systems [43]. Here, residues from helix III again were found to participate in domain-domain interaction. Other reports have also shown that helix III can be highly mobile in other carrier proteins [40], indicating that they may play roles in mediating protein interactions for these systems, too.

In both EntB and EntF, the iron-dependent selection could be utilized to identify residues involved in slow catalytic steps. It is difficult to determine which step of the enterobactin synthesis cascade is rate limiting; however, the selection is likely able to assay only steps that can be rate limiting. Structural studies (NMR, X-ray crystallography) are required to gain a complete understanding of domain-domain interactions in the enterobactin synthetase.

Thiolation domains must be versatile to dock with distinct partner proteins, and the pantetheinyl arm can swivel over an arc of 120 degrees to populate distinct T domain conformers [32, 43], movements that undoubtedly affect recognition by partner proteins. The conformational rearrangements in T domains are perhaps analogous to mobile conformations of switch regions in G proteins that alter recognition by partner protein components. It is likely that T domains are workhorse scaffolds in natural product assembly lines where the pantetheinyl arm mobility, conformational dynamics, and surface residue recognition will control growing chain flux through these way stations.

Significance

Carrier protein domains, also known as thiolation (T) domains, are 8–10 kDa protein way stations in natural product assembly lines on which growing chains are

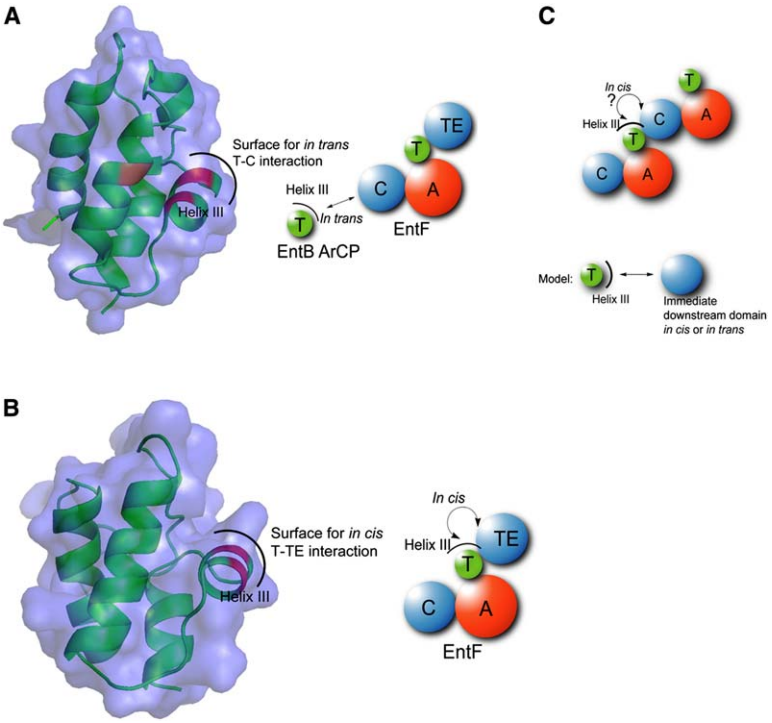

Figure 7. Model for Interaction between a T Domain and Its Downstream Partner

(A) The surface (blue) and ribbon (green) representation of EntB T domain (structure prepared from PDB code: 2FQ1) in trans interaction with EntF C domain. The helix III residues (F264 and A268) which are responsible for interaction with EntF C domain are shown in red. The helix II residue M249 is shown in orange.

(B) EntF T domain (homology model) in cis interaction with EntF TE domain. The helix III residues (G1027 and M1030), which are responsible for T-TE interaction, are shown in red.

(C) A model of helix III as communication motif for T-downstream domain interaction.

covalently tethered during elongation. Thus, T domains are information-rich scaffolds for protein-protein interactions in NRP biosynthesis. In this study, we characterized helix III residues on the T domain of EntF in Ent synthetase as the specific interaction surface for in cis T-TE (thioesterase domain) interaction. Furthermore, comparing the recently defined interaction surface on EntB for in trans T-C (condensation domain) interaction with the results presented here, we propose a general model for interaction between a T domain and the immediate downstream domain. Understanding the protein recognition features in natural product synthetases will provide useful information for engineering noncognate protein-protein interactions involving T domains and facilitate manipulation of NRPS/PKS modules for combinatorial biosynthesis.

Experimental Procedures

Production of a Homology Model for EntF T Domain

The T domain of EntF (residues 960–1047) was aligned with TycC3-PCP (PDB code: 1DNY) with the ClustalW algorithm. A homology model was generated by Swiss-Pdb Viewer (http://swissmodel.expasy.org/spdbv/) and refined by SWISS-MODEL (http://swissmodel.expasy.org/). All structural figures were prepared with Pymol (DeLano Scientific, http://pymol.sourceforge.net/).

Library Construction and Selection for Enterobactin Production

For each library, an inactive template based on wild-type EntF construct pER311A [28] was generated by the SOE method [51]. The inactive templates contained tandem TAA stop codons followed by a unique restriction site SacI in the region of EntF T domain to be randomized. These inactive templates were used for full plasmid replication with the primers 5′-GCG CTT GGC GGT CAT TCG **SYT SYT** GCA **RYG RMA** CTG GCA **SMA** CAG TTA AGT CGG CAG GTT-3′ for helix II library, 5′-CGC CAG GTG ACG CCG GGG **SMA GYT RYG GYT SMA** TCA ACT GTC GCC AAA CTG-3′ for helix III library, and 5′-CAG TTA AGT CGG CAG GTT GCA **SST SMA GYT RCT SCA** GST CAA GTG ATG GTC GCG TCA-3′ for loop II/helix III library, respectively (sites of randomization indicated in bold; DNA degeneracies are represented as: K = G/T, M = A/C, R = A/G, S = G/C, Y = C/T). DpnI and SacI were used to destroy the templates. Library DNA were transformed into electrocompetent *entF*::*cat* [28] cells and plated onto minimal media in which iron was sequestered by the addition of 100 μM 2,2′-dipyridyl. The transformats were allowed to grow for 24 hr, and the largest colonies were isolated and sequenced. Sequencing was performed at the Dana Farber Cancer Institute Molecular Biology Core Facilities.

Site-Directed Mutagenesis, Protein Expression, and Purification

The EntF site-directed mutants L1007A, K1011A, G1027A, and M1030A were constructed by the SOE method [51]. The generation of H1271A and H138A were previously described [28]. The overexpression and purification of EntF (wild-type and mutants), EntE, EntB-ArCP, EntD, and Sfp were performed as reported [28, 37, 52]. Protein concentrations were determined by Bradford assay.

Phosphopantetheinylation Assays

Phosphopantetheinylation was measured by incorporation of radiolabeled [^{3}H]CoASH onto EntF (wt and mutants). Reactions were performed under the following condition: 75 mM Tris (pH 7.5), 10 mM $MgCl_2$, 0.5 mM Tris(2-Carboxyethyl) phosphine (TCEP), 6 μM EntF (wt and mutants), 30 μM [^{3}H]CoASH (66.8 Ci/mol, prepared previously in [53]), and they were initiated by the addition of 1 μM EntD. Reactions were quenched with of 10% (wt/vol) TCA, and then BSA (100 mg) was added as a carrier. The protein pellet was washed with 10% (wt/vol) TCA and resuspended in formic acid, and the amount of radioactive label was measured by liquid scintillation counting.

Enterobactin Reconstitution Assay

Holo EntB-ArCP and EntF were prepared by incubating the apo proteins with 300 nM Sfp and 500 μM CoASH in 75 mM Tris (pH 7.5), 10 mM $MgCl_2$, and 0.5 mM TCEP for 20 min. The enterobactin reconstitution assay was performed as in [37] and modified to the following condition: 75 mM Tris (pH 7.5), 10 mM $MgCl_2$, 0.5 mM TCEP, 500 μM DHB, 1 mM L-serine, 10 mM ATP, 300 nM EntE, 15 μM holo EntB-ArCP, 100 nM holo EntF (wt or mutants). Reaction

progress was monitored by high-performance liquid chromatography (HPLC) with water/acetonitrile/trifluoroacetic acid mobile phases. Duplicate experiments were performed to determine initial rates for enterobactin reconstitution.

Ser Incorporation Assay

Reactions were performed under the following condition: 75 mM Tris (pH 7.5), 10 mM $MgCl_2$, 0.5 mM TCEP, 5 μM holo EntF (wt and mutants), 200 μM [^{14}C] L-Ser (52.38 Ci/mol, Sigma), and they were initiated by the addition of 10 mM ATP. The measurement of the amount of radioactive label on proteins was performed the same as that described in the Phosphopantetheinylation Assay section. Experiments were performed in duplicates.

Condensation Assay

Holo form EntF C-A-T (wt and mutants) proteins were prepared as above. The reaction mixture containing 75 mM Tris (pH 7.5), 10 mM $MgCl_2$, 0.5 mM TCEP, 5 μM holo EntF C-A-T (wt and mutants), 10 μM EntB-ArCP, 900 nM EntE, 100 μM [^{14}C] L-Ser(52.38 Ci/mol, Sigma), and 10 mM ATP were preincubated for 5 min to allow Ser loading. The condensation reactions were started by adding 500 μM DHB. Reactions were quenched with in 15 s and washed with 10% TCA. The protein pellets were resuspended in 100 ul 0.5 M KOH. After 10 min incubation at room temperature, which allows the release of Ser or DHB-Ser from proteins, 10 ul of 50% TFA (trifluoroacetic acid) was added to acidify the mixture. Precipitation was removed by centrifugation and supernatants were analyzed by HPLC. Flow-through radioactivity was monitored by using a Radioisotope Detector β-RAM Model 3 (Beckman).

Acyl Transfer Assay

Reactions were performed under this condition: 75 mM Tris (pH 7.5), 10 mM $MgCl_2$, 0.5 mM TCEP, 75 μM 1-[^{14}C]acetyl-CoA (31.10 Ci/mol, Amersham Pharmacia), and 6 μM EntF (wt and mutants). Reactions were started by adding 300 nM Sfp. Reactions were quenched, and the amount of radioactive label was measured as described in the Phosphopantetheinylation Assay section.

Supplemental Data

Supplemental Data include the statistical results of combinatorial alanine scanning and rates of enterobactin production for EntF (wt and mutants) and are available at http://www.chembiol.com/cgi/content/full/13/8/869/DC1/.

Acknowledgments

This research was supported by the National Institutes of Health (AI042738, GM020011, and GM047467). J.R.L. is supported by a post-doctoral fellowship from the Helen Hay Whitney Foundation. We thank Michael Fischbach, Ellen Yeh, and Hening Lin for helpful discussion and critical reading of this manuscript.

Received: April 24, 2006
Revised: June 8, 2006
Accepted: June 15, 2006
Published: August 25, 2006

References

1. Cane, D.E., Walsh, C.T., and Khosla, C. (1998). Harnessing the biosynthetic code: combinations, permutations, and mutations. Science *282*, 63–68.
2. Donadio, S., Staver, M.J., McAlpine, J.B., Swanson, S.J., and Katz, L. (1991). Modular organization of genes required for complex polyketide biosynthesis. Science *252*, 675–679.
3. Watanabe, K., Rude, M.A., Walsh, C.T., and Khosla, C. (2003). Engineered biosynthesis of an ansamycin polyketide precursor in *Escherichia coli*. Proc. Natl. Acad. Sci. USA *100*, 9774–9778.
4. Hubbard, B.K., and Walsh, C.T. (2003). Vancomycin assembly: nature's way. Angew. Chem. Int. Ed. Engl. *42*, 730–765.
5. Motamedi, H., and Shafiee, A. (1998). The biosynthetic gene cluster for the macrolactone ring of the immunosuppressant FK506. Eur. J. Biochem. *256*, 528–534.
6. Schwecke, T., Aparicio, J., Molnar, I., Konig, A., Khaw, L., Haycock, S., Oliynyk, M., Caffrey, P., Cortes, J., Lester, J., et al. (1995). The biosynthetic gene cluster for the polyketide immunosuppressant rapamycin. Proc. Natl. Acad. Sci. USA *92*, 7839–7843.
7. Tang, L., Shah, S., Chung, L., Carney, J., Katz, L., Khosla, C., and Julien, B. (2000). Cloning and heterologous expression of the epothilone gene cluster. Science *287*, 640–642.
8. Shen, B., Du, L., Sanchez, C., Edwards, D.J., Chen, M., and Murrell, J.M. (2002). Cloning and characterization of the bleomycin biosynthetic gene cluster from *Streptomyces verticillus* ATCC15003. J. Nat. Prod. *65*, 422–431.
9. Walsh, C.T., Gehring, A.M., Weinreb, P.H., Quadri, L.E., and Flugel, R.S. (1997). Post-translational modification of polyketide and nonribosomal peptide synthases. Curr. Opin. Chem. Biol. *1*, 309–315.
10. Schweizer, E., and Hofmann, J. (2004). Microbial type I fatty acid synthases (FAS): major players in a network of cellular FAS systems. Microbiol. Mol. Biol. Rev. *68*, 501–517.
11. Staunton, J., and Weissman, K.J. (2001). Polyketide biosynthesis: a millennium review. Nat. Prod. Rep. *18*, 380–416.
12. Marahiel, M.A., Stachelhaus, T., and Mootz, H.D. (1997). Modular peptide synthetases involved in nonribosomal peptide synthesis. Chem. Rev. *97*, 2651–2674.
13. White, S.W., Zheng, J., Zhang, Y.-M., and Rock, C.O. (2005). The structural biology of type II fatty acid biosynthesis. Annu. Rev. Biochem. *74*, 791–831.
14. Du, L., and Shen, B. (1999). Identification and characterization of a type II peptidyl carrier protein from the bleomycin producer *Streptomyces verticillus* ATCC 15003. Chem. Biol. *6*, 507–517.
15. Tsuji, S.Y., Wu, N., and Khosla, C. (2001). Intermodular communication in polyketide synthases: comparing the role of protein-protein interactions to those in other multidomain proteins. Biochemistry *40*, 2317–2325.
16. Kumar, P., Li, Q., Cane, D.E., and Khosla, C. (2003). Intermodular communication in modular polyketide synthases: structural and mutational analysis of linker mediated protein-protein recognition. J. Am. Chem. Soc. *125*, 4097–4102.
17. Chen, H., and Walsh, C.T. (2001). Coumarin formation in novobiocin biosynthesis: [beta]-hydroxylation of the aminoacyl enzyme tyrosyl-S-NovH by a cytochrome P450 NovI. Chem. Biol. *8*, 301–312.
18. Patel, H.M., and Walsh, C.T. (2001). In vitro reconstitution of the *Pseudomonas aeruginosa* nonribosomal peptide synthesis of pyochelin: characterization of backbone tailoring thiazoline reductase and *N*-methyltransferase activities. Biochemistry *40*, 9023–9031.
19. Patel, H.M., Tao, J., and Walsh, C.T. (2003). Epimerization of an *L*-cysteinyl to a *D*-cysteinyl residue during thiazoline ring formation in siderophore chain elongation by pyochelin synthetase from *Pseudomonas aeruginosa*. Biochemistry *42*, 10514–10527.
20. Vaillancourt, F.H., Yeh, E., Vosburg, D.A., O'Connor, S.E., and Walsh, C.T. (2005). Cryptic chlorination by a non-haem iron enzyme during cyclopropyl amino acid biosynthesis. Nature *436*, 1191–1194.
21. Raymond, K.N., Dertz, E.A., and Kim, S.S. (2003). Enterobactin: an archetype for microbial iron transport. Proc. Natl. Acad. Sci. USA *100*, 3584–3588.
22. Crosa, J.H., and Walsh, C.T. (2002). Genetics and assembly line enzymology of siderophore biosynthesis in bacteria. Microbiol. Mol. Biol. Rev. *66*, 223–249.
23. Rusnak, F., Faraci, W.S., and Walsh, C.T. (1989). Subcloning, expression, and purification of the enterobactin biosynthetic enzyme 2,3-dihydroxybenzoate-AMP ligase: demonstration of enzyme-bound (2,3-dihydroxybenzoyl)adenylate product. Biochemistry *28*, 6827–6835.
24. Rusnak, F., Liu, J., Quinn, N., Berchtold, G.A., and Walsh, C.T. (1990). Subcloning of the enterobactin biosynthetic gene entB: expression, purification, characterization, and substrate specificity of isochorismatase. Biochemistry *29*, 1425–1435.
25. Gehring, A.M., Bradley, K.A., and Walsh, C.T. (1997). Enterobactin biosynthesis in *Escherichia coli*: isochorismate lyase (EntB) is a bifunctional enzyme that is phosphopantetheinylated by EntD

and then acylated by EntE using ATP and 2,3-dihydroxybenzoate. Biochemistry *36*, 8495–8503.

26. Reichert, J., Sakaitani, M., and Walsh, C.T. (1992). Characterization of EntF as a serine-activating enzyme. Protein Sci. *1*, 549–556.
27. Ehmann, D.E., Shaw-Reid, C.A., Losey, H.C., and Walsh, C.T. (2000). The EntF and EntE adenylation domains of *Escherichia coli* enterobactin synthetase: sequestration and selectivity in acyl-AMP transfers to thiolation domain cosubstrates. Proc. Natl. Acad. Sci. USA *97*, 2509–2514.
28. Roche, E.D., and Walsh, C.T. (2003). Dissection of the EntF condensation domain boundary and active site residues in nonribosomal peptide synthesis. Biochemistry *42*, 1334–1344.
29. Shaw-Reid, C.A., Kelleher, N.L., Losey, H.C., Gehring, A.M., Berg, C., and Walsh, C.T. (1999). Assembly line enzymology by multimodular nonribosomal peptide synthetases: the thioesterase domain of *E. coli* EntF catalyzes both elongation and cyclolactonization. Chem. Biol. *6*, 385–400.
30. Tang, Y., Lee, T.S., Kobayashi, S., and Khosla, C. (2003). Ketosynthases in the initiation and elongation modules of aromatic polyketide synthases have orthogonal acyl carrier protein specificity. Biochemistry *42*, 6588–6595.
31. Lai, J.R., Fischbach, M.A., Liu, D.R., and Walsh, C.T. (2006). A protein interaction surface in nonribosomal peptide synthesis mapped by combinatorial mutagenesis and selection. Proc. Natl. Acad. Sci. USA *103*, 5314–5319.
32. Weber, T., Baumgartner, R., Renner, C., Marahiel, M.A., and Holak, T.A. (2000). Solution structure of PCP, a prototype for the peptidyl carrier domains of modular peptide synthetases. Structure *8*, 407–418.
33. Parris, K.D., Lin, L., Tam, A., Mathew, R., Hixon, J., Stahl, M., Fritz, C.C., Seehra, J., and Somers, W.S. (2000). Crystal structures of substrate binding to *Bacillus subtilis* holo-(acyl carrier protein) synthase reveal a novel trimeric arrangement of molecules resulting in three active sites. Structure *8*, 883–895.
34. Finking, R., Mofid, M.R., and Marahiel, M.A. (2004). Mutational analysis of peptidyl carrier protein and acyl carrier protein synthase unveils residues involved in protein-protein recognition. Biochemistry *43*, 8946–8956.
35. Weiss, G.A., Watanabe, C.K., Zhong, A., Goddard, A., and Sidhu, S.S. (2000). Rapid mapping of protein functional epitopes by combinatorial alanine scanning. Proc. Natl. Acad. Sci. USA *97*, 8950–8954.
36. Lambalot, R.H., Gehring, A.M., Flugel, R.S., Zuber, P., LaCelle, M., Marahiel, M.A., Reid, R., Khosla, C., and Walsh, C.T. (1996). A new enzyme superfamily—the phosphopantetheinyl transferases. Chem. Biol. *3*, 923–936.
37. Gehring, A.M., Mori, I., and Walsh, C.T. (1998). Reconstitution and characterization of the *Escherichia coli* enterobactin synthetase from EntB, EntE, and EntF. Biochemistry *37*, 2648–2659.
38. Kohli, R.M., and Walsh, C.T. (2003). Enzymology of acyl chain macrocyclization in natural product biosynthesis. Chem. Commun. (Camb.) 297–307.
39. Kim, Y., and Prestegard, J.H. (1990). Refinement of the NMR structures for acyl carrier protein with scalar coupling data. Proteins *8*, 377–385.
40. Li, Q., Khosla, C., Puglisi, J.D., and Liu, C.W. (2003). Solution structure and backbone dynamics of the holo form of the frenolicin acyl carrier protein. Biochemistry *42*, 4648–4657.
41. Crump, M.P., Crosby, J., Dempsey, C.E., Parkinson, J.A., Murray, M., Hopwood, D.A., and Simpson, T.J. (1997). Solution structure of the actinorhodin polyketide synthase acyl carrier protein from *Streptomyces coelicolor* A3(2). Biochemistry *36*, 6000–6008.
42. Wong, H.C., Liu, G., Zhang, Y.M., Rock, C.O., and Zheng, J. (2002). The solution structure of acyl carrier protein from *Mycobacterium tuberculosis*. J. Biol. Chem. *277*, 15874–15880.
43. Koglin, A., Mofid, M.R., Lohr, F., Schafer, B., Rogov, V.V., Blum, M.M., Mittag, T., Marahiel, M.A., Bernhard, F., and Dotsch, V. (2006). Conformational switches modulate protein interactions in peptide antibiotic synthetases. Science *312*, 273–276.
44. Drake, E.J., Nicolai, D.A., and Gulick, A.M. (2006). Structure of the EntB multidomain nonribosomal peptide synthetase and functional analysis of its interaction with the EntE adenylation domain. Chem. Biol. *13*, 409–419.
45. Carreras, C.W., Gehring, A.M., Walsh, C.T., and Khosla, C. (1997). Utilization of enzymatically phosphopantetheinylated acyl carrier proteins and acetyl-acyl carrier proteins by the actinorhodin polyketide synthase. Biochemistry *36*, 11757–11761.
46. Schwecke, T., Aparicio, J.F., Molnar, I., Konig, A., Khaw, L.E., Haydock, S.F., Oliynyk, M., Caffrey, P., Cortes, J., Lester, J.B., et al. (1995). The biosynthetic gene cluster for the polyketide immunosuppressant rapamycin. Proc. Natl. Acad. Sci. USA *92*, 7839–7843.
47. Keller, N.P., Turner, G., and Bennett, J.W. (2005). Fungal secondary metabolism—from biochemistry to genomics. Nat. Rev. Microbiol. *3*, 937–947.
48. Mootz, H.D., and Marahiel, M.A. (1997). The tyrocidine biosynthesis operon of *Bacillus brevis*: complete nucleotide sequence and biochemical characterization of functional internal adenylation domains. J. Bacteriol. *179*, 6843–6850.
49. Garneau, S., Dorrestein, P.C., Kelleher, N.L., and Walsh, C.T. (2005). Characterization of the formation of the pyrrole moiety during clorobiocin and coumermycin A1 biosynthesis. Biochemistry *44*, 2770–2780.
50. Aguilar, R.C., and Wendland, B. (2003). Ubiquitin: not just for proteasomes anymore. Curr. Opin. Cell Biol. *15*, 184–190.
51. Ho, S.N., Hunt, H.D., Horton, R.M., Pullen, J.K., and Pease, L.R. (1989). Site-directed mutagenesis by overlap extension using the polymerase chain reaction. Gene *77*, 51–59.
52. Quadri, L.E., Weinreb, P.H., Lei, M., Nakano, M.M., Zuber, P., and Walsh, C.T. (1998). Characterization of Sfp, a *Bacillus subtilis* phosphopantetheinyl transferase for peptidyl carrier protein domains in peptide synthetases. Biochemistry *37*, 1585–1595.
53. Lambalot, R.H., and Walsh, C.T. (1995). Cloning, overproduction, and characterization of the *Escherichia coli* holo-acyl carrier protein synthase. J. Biol. Chem. *270*, 24658–24661.